View metadata, citation and similar papers at core.ac.uk
brought to you by CORE
provided by Repository@USM

SYNTHESIS OF TiO_2 NANOTUBE ARRAYS AND PREPARATION OF AGAR BASED GEL POLYMER ELECTROLYTE FOR DYE-SENSITIZED SOLAR CELL

by

JEREMY KOH CHEE HAO

Thesis submitted in fulfillment of the requirements
for the degree of
Master of Science

May 2011

ACKNOWLEDGEMENT

I would like to express my deepest appreciation to my main supervisor, Associate Prof. Dr. Ahmad Azmin Mohamad, and to my co-supervisor, Prof. Dr. Hj. Zainal Arifin Ahmad, who supported me throughout the completion of my thesis with their patience and knowledge. The level of my master's degree is due to their encouragement and effort. This thesis, too, would not have been written or completed without their help. Their constant guidance and unconditional support have always been inspiring.

I am also grateful to all the academic and technical staff of the School of Materials and Minerals Resources Engineering, USM, especially Mr. Suhaimi Sulong, for their kind assistance and patience throughout my experimental works. My appreciation also goes to my postgraduate colleagues, Mohd Najmi Masri, Muhamad Firdaus Mohd Nazeri, Aliyah Jamaludin, and Siti Salwa Alias, for their assistance and moral support throughout the completion of this thesis. I also express my thanks to the USM Fellowship and Research University Postgraduate Research Grant Scheme for their financial support and funding.

Finally, my gratitude goes to my family, especially my mother, Esther Khew, aunt, cousin brother, sister, Tan Wee Ching, and my beloved friends. To all whom I did not mention above, please accept my gratitude for your invaluable contributions and encouragement towards my goal and achievement. Without you all, this thesis would not have materialized. I am honored to be associated with all of you.

JEREMY KOH CHEE HAO

LIST OF CONTENTS

LIST OF TABLES

Pages

LIST OF FIGURES

LIST OF ABBREVIATIONS

$-(CH(-CH_3)CH_2O)_n-$	Poly(propylene oxide)
$-(CH_2C(-CH_3)(-COOCH_3))_n-$	Poly(methyl methacrylate)
$-(CH_2CF_2)_n-$	Poly(vinylidene fluoride)
$-(CH_2-CH(-CN))_n-$	Poly(acrylonitrile)
$-(CH_2-CH)-$	Poly(vinylidene fluoride-hexafluoropropylene)
$-(CH_2CH_2O)_n-$	Poly(ethylene oxide)
$-(CH_2CHCl)_n-$	Poly(vinyl chloride)
(TiO_2^{6-})	Titanium Dioxide Octahedrals
$[TiF_6]^{2-}$	Fluoride Complex
AC	Alternating Current
BL	Γ-Butyrolactone
CeO_2	Cerium Oxide
DEC	Diethyl Carbonate
DMC	Dimethyl Carbonate
DSSC	Dye Sensitized Solar Cell
Dye^+	Excited Dye
e^-	Free Electron
EC	Ethylene Carbonate
EDX	Energy Dispersive X-ray Spectroscopy
EIS	Electrochemical Impedance Spectroscopy
F^-	Fluoride Ion
FESEM	Field Emission Scanning Electron Microscopy

FRA	Frequency Response Analyzer
FTO	Fluorine Tin Oxide
GPE	Gel Polymer Electrolyte
GPES	General Purpose Electrochemical System
H^+	Hydrogen Ion
H_2O	Water
H_3PO_4	Phosphoric Acid
HCl	Hydrochloric Acid
HF	Hydrofluoric Acid
I^-	Iodide Ion
I_2	Iodine
I_3^-	Triiodide Ion
In_2O_3	Indium Oxide
ITO	Indium Tin Oxide
I-V	Current-Voltage
LPE	Liquid Polymer Electrolyte
LSV	Linear Sweep Voltammetry
M	Metal
$M(OH)_4$	Metal Tetrahydroxide
M^{4+}	Metal Ion
MnO	Manganese Oxide
MO_2	Metal Oxide
N719	Bis(tetrabutylammonium)-cis-(dithiocyanato)-N,N0-bis(4-carboxylate-40-carboxylic acid-,20-bipyridine) ruthenium (II)

Na	Sodium
NaF	Sodium Fluoride
NaI	Sodium Iodide
NaOH	Sodium Hydroxide
Nb_2O_5	Niobium Pentoxide
NH_4F	Ammonium Fluoride
O	Oxygen
O_2	Oxygen Gas
O^{2-}	Oxygen Ion
OH	Hydroxyl
PbO_2	Lead Oxide
PC	Propylene Carbonate
Pt	Platinum
PTFE	Poly-tetra-fluoro-ethylene
QSSC	Quasi-Solid-State Solar Cell
SEM	Scanning Electron Microscopy
SnO_2	Tin Oxide
SPE	Solid Polymer Electrolyte
$SrTiO_3$	Strontium Titanium Oxide
SS	Stainless Steel
TEM	Transmission Electron Microscopy
Ti	Titanium
Ti^{4+}	Titanium Ion
TiO_2	Titanium dioxide
XRD	X-ray Diffraction

ZnO	Zinc Oxide

LIST OF SYMBOLS

A	Intact Area of Electrolyte
E_a	Activation Energy
f	Frequency
I	Current
I_{sc}	Short Circuit Current
k	Boltzmann Constant
r	Radius of Spherical
R	Mass Loss Rate
R_b	Bulk Resistance
T	Temperature
t	Time
V	Voltage
V_{oc}	Open Circuit Voltage
Z'	Real Impedance
Z"	Imaginary Impedance
σ	Ionic Conductivity
σ_o	Preexponential Factor
t_e	Thickness of Electrolyte
j	Imaginary Number

SINTESIS TIUBNANO TiO_2 DAN PENYEDIAAN ELEKTROLIT GEL POLIMER BERASASKAN AGAR UNTUK SEL SURIA BERPEKAAN PENCELUP

ABSTRAK

Dalam kajian ini, katod-udara digunakan untuk menghasilkan tiubnano TiO_2. Kesan pH dan voltan dalam pengubahsuaian morfologi tiubnano TiO_2 telah dikaji. Tambahan pula, kestabilan katod udara dalam pelbagai keadaan penganodan juga dikaji buat pertama kalinya. Keputusan awal menunjukkan bahawa tiubnano penjajaran TiO_2 dibentuk sepadan dengan yang disintesis oleh elektrod platinum dalam keadaan yang sama. Panjang dan diameter tiubnano TiO_2 diperolehi dalam lingkungan 1.0-2.0 μm dan 50-100 nm, masing-masing. Katod-udara ditemui menunjukkan kadar kehilangan berat yang rendah, dengan nilai antara 0.04-0.08 mg cm^{-2} h^{-1}. Tiubnano TiO_2 yang telah dianodkan berbentuk dalam struktur amorfus pada 20 dan 30 V, walaupun struktur anatase dan rutile boleh dibentuk pada 40-70 V. Elektrolit gel polimer (GPE) disediakan berasaskan agar BACTO disediakan sebagai perumah kepada elektrolit cair untuk menambahkan kestabilan mekanikal. Kepekatan NaI (0-2 M) dan I_2 (0-70 μL) diubah untuk mendapatkan kombinasi NaI dan I_2 dengan konduktiviti terbaik disamping mengekalkan kekuatan mekanikal terbaik bagi GPE tersebut. GPE pada komposisi BACTO + 1.6 M NaI + 50 μL I_2 telah mencatatkan bacaan konduktiviti ionik optimum sebanyak 1.22×10^{-3} S cm^{-1}. Kajian konduktiviti-suhu menyatakan bahawa GPE adalah terma-aktif dan Arrhenius manakala keputusan voltametri sapuan lurus menunjukkan bahawa tingkap keupayaan untuk sampel GPE adalah antara 1.85-1.89 V pada suhu 298-353 K. Plot arus-voltan menunjukkan tindakbalas fotoarus dari QSSC yang difabrikasi.

SYNTHESIS OF TiO_2 NANOTUBE ARRAYS AND PREPARATION OF AGAR BASED GEL POLYMER ELECTROLYTE FOR DYE-SENSITIZED SOLAR CELL

ABSTRACT

In the current study, air-cathode is used to synthesize titanium dioxide (TiO_2) nanotube arrays. Effect of pH and voltage in tailoring the morphologies of TiO_2 nanotube arrays is investigated. Furthermore, the stability of air-cathodes at different anodization conditions is investigated for the first time. Preliminary results show that self-aligned TiO_2 nanotube arrays formed is comparable to those synthesized by platinum electrode under similar conditions. The lengths and diameters of TiO_2 nanotube arrays are in the range of 1.0-2.2 μm and 50-100 nm, respectively. Air-cathodes are found to have low value of mass loss rates, with mean values in the range of 0.04-0.08 mg cm^{-2} h^{-1}. As-anodized TiO_2 nanotube arrays are formed as amorphous structures at 20 and 30 V, although anatase and rutile structures could be formed at 40-70 V. Gel polymer electrolyte (GPE) is prepared based on BACTO agar as polymer host encapsulating liquid electrolyte to introduce mechanical stability. Concentrations of NaI (0-2 M) and I_2 (0-70 μL) are varied to obtain a combination of NaI + I_2 with the best conductivity while maintaining good mechanical strength on the GPE. The GPE is optimized with BACTO + 1.6 M NaI + 50 μL I_2 recording ionic conductivity of 1.22×10^{-3} S cm^{-1}. Conductivity-temperature study reveals that the GPEs are thermally activated and Arrhenius while linear sweep voltammetry results suggest that the operating potential window for the GPEs sample are between 1.85–1.89 V at temperature 298–353 K. Finally, the current-voltage plot of assembled QSSC shows photocurrent response under illumination.

CHAPTER 1

INTRODUCTION

1.1 Introduction

Titanium dioxide (TiO_2) is a semiconducting material that exhibits great electrical properties. The versatility of TiO_2, which appears as various structures, has made it one of the leading materials in solar cell technology. Tubular nanostructured TiO_2 has extensive applications in solar cells because of its high surface-to-volume ratio, which results in high surface activity and high sensitivity. To obtain one-dimensional (1-D) TiO_2 nanotube arrays, suitable synthesis must be employed. Among all the reported synthesis methods, anodic oxidation, also known as metal anodization, is widely regarded as the best technique to synthesize TiO_2 nanotube arrays.

With metal anodization, the choice of material used is crucial because the cathode would indirectly affect surface morphologies and structure of the TiO_2 nanotube arrays. Hence, questions have been raised on the cathode material that would best fit titanium anodization. Platinum (Pt) electrode has always been the primary choice because of its inertness in harsh processing conditions. However, Pt electrode can be highly expensive, which greatly restricts its design.

Successful oxide synthesis employing air-cathode (Tan and Mohamad, 2010) has been considered as a replacement of Pt in its role. Although the nature of oxide formation is slightly different from metal anodization, both systems are electrochemically similar. In addition, air-cathode is relatively cheaper compared to

Pt and has high design flexibility. Commercially, air-cathode is available in several shapes and dimensions. Thus, it can be easily modified to accommodate the metal anodization process. Its high durability and infinitely useful life reduce the need for maintenance. The biggest advantage of air-cathode would be its high surface area for metal anodization.

Nanostructured TiO_2, in the form of nanotubes in particular, is the overwhelming favorite photoanode of dye-sensitized solar cell (DSSC). The fabrication of DSSC based on TiO_2 as the photoanode is promising; however, it has yet to fulfill its potential due to some complications from constituents within the DSSC. Most notably, problems that are prevalent with the use of liquid electrolyte in DSSC, such as leakage, solvent evaporation, high-temperature instability, photochemical degradation, and sealing (Mohamad and Arof, 2007) have greatly dampened the performance of DSSC. Thus, embedding a polymer host, such as agar, to provide mechanical stability to the liquid-based electrolyte, could curb the aforementioned issues.

As a natural polymer, agar is abundantly available in nature and does not cause pollution to the environment because of its low toxicity and biodegradation properties. In addition, agar is relatively low-cost and does not involve complicated synthesis routes compared with synthetic polymers. Thus, agar is highly favorable as polymer host for liquid-based electrolyte in the fabrication of DSSC.

These implications have led to further development of Ti anodization technique, as well as the applicability of agar-based electrolyte in dye-sensitized solar cell (DSSC) system.

1.2 Problem Statement

As previously mentioned, air-cathode is as a candidate to replace Pt as cathode material during metal anodization. However, the ability of air-cathode to synthesize TiO_2 nanotube arrays is yet to be justified. Furthermore, the effect of the cathode material in metal anodization on the properties of the resulting nanotube arrays is still insufficient, especially in TiO_2 nanotube arrays formation. Thus, study on the effect of cathode material on the structures and properties of formed TiO_2 nanotube arrays is necessary.

Agar has been previously reported as a possible polymer host because of environmental issues as well as its intrinsic properties (Raphael *et al.*, 2010). Although the application of agar-based GPE has attracted great interest, the rich nutrients within agar could damage its long-term application in DSSC technology. The presence of detrimental ions, debris, and mineral salts would encourage the growth of microorganisms, which would in turn deteriorate the performance of DSSC. Thus, a polymer host that possesses the advantages of agar while keeping the contaminants at a very low level would be ideal.

1.3 Objectives

The main objectives of this work are as follows:

i. To study the applicability of air-cathode as the cathode material in the synthesis of TiO_2 nanotube arrays via anodization process;
ii. To study the effect of sodium iodide (NaI) and iodine (I_2) on the conductivity of BACTO agar-based GPE; and
iii. To fabricate DSSC based on prepared TiO_2 nanotube arrays together with BACTO agar-based GPE and to study its performance.

1.4 Scope of Work

This project covers the following: (i) the synthesis of TiO_2 nanotube arrays via anodization, with air-cathode as the cathode material; (ii) preparation of BACTO agar-based redox electrolyte, including the effect of conducting elements of NaI and I_2 on the conductivity of GPE; and (iii) fabrication and characterization of DSSC to examine the workability of synthesized TiO_2 photoanode and BACTO agar-based GPE combination.

CHAPTER 2

LITERATURE REVIEW

2.1 Introduction

This chapter focuses on two main topics. The first involves the synthesis of titanium dioxide (TiO_2) nanotubes employing air-cathode as the cathode electrode. The second involves the review of gel polymer electrolyte (GPE). Toward the end of this chapter, the roles of the above two materials in dye-sensitized solar cell (DSSC) are briefly explained.

2.2 Titanium Dioxide (TiO_2)

Titanium dioxide (TiO_2) belongs to the family of transition metal oxides (Greenwood and Earnshaw, 1997). TiO_2, also commonly known as titanium (IV) oxide or titania, is naturally present in the oxide of titanium (Ti) with chemical formula of TiO_2. TiO_2 is a wide band gap semiconductor with band gap energy ranging from 3.00 to 3.21 eV. It is biologically and chemically stable/inert, leading to its a wide range of applications. Traditionally, it is used as a white pigment in paints, plastic, and paper, which are the major end-use sectors of TiO_2. However, with the development of science and technology, the application of TiO_2 in minor end-use sectors has blossomed in recent years. By careful handling of the material, TiO_2 is deemed harmless to the human body and chemically stable with respect to chemical corrosion. Recently, TiO_2 has also been reported in food application (Chorianopoulos *et. al.*, 2011; Tahergorabi *et. al.*, 2010). The usage of TiO_2 is not

only limited to those previously mentioned. It is also one of the most exploited materials in more sophisticated high-technology applications. The semiconducting properties of TiO_2, which respond to light rays, and its subsequent application in photoelectrochemical cell are some of its prime advantages. Table 2.1 highlights some of the application of TiO_2 nanotubes.

Table 2.1: Some applications of TiO_2 nanotubes.

TiO_2 nanotubes application	Reference
Photovoltaic	Grimes and Mor (2009); Jiang *et. al.* (2001)
Sensors	Varghese *et. al.* (2006); Mor *et. al.* (2006)
Catalysis	Macak *et. al.* (2007); Gaudino *et. al.* (2005)
Biomedical	Brunette *et. al.* (2001)
Ceramics	Kingery *et. al.* (1976); Uchino (2000)
Interference coating, optical devices	Lai *et. al.* (2005)

2.2.1 Synthesis Methods of TiO_2 Nanotubes

TiO_2 nanotubes with high surface-to-volume ratio, ion-changeable ability, and photocatalytic ability have been considered for extensive applications. To date, a number of synthesis methods to produce nanostructure TiO_2 have been reported. The trend of synthesis approaches for TiO_2 nanotubes is demonstrated in Figure 2.1.

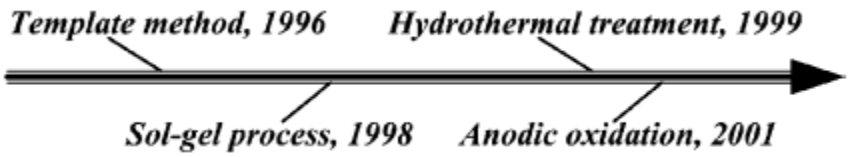

Figure 2.1: The developing trend of synthesis approach for TiO_2 nanotubes (Ou and Lo, 2007).

Synthesis of TiO_2 nanotubes was first reported by Hoyer (1996) via template-assisted method. Since then, electrochemical synthesis has become the preferred means of synthesizing TiO_2 nanotubes. Table 2.2 lists some of the more conventional ways to form nanostructured TiO_2. Each of these fabrication methods has its unique advantages and functional features. Among the aforementioned synthesis methods, sol-gel and hydrothermal synthesis are the more popular and widely adopted technique to produce TiO_2 nanotubes. These successful techniques have been extensively investigated because of their feasibility in widespread applications.

Table 2.2: Methods for formation of nanoscale TiO_2.

Formation method	Reference
Anodic oxidation	Cai *et. al.* (2006); Schmuki *et. al.* (2006)
Electrochemical lithography	Lai *et. al.* (2008)
Sol-gel processing	Fang *et. al.* (2010); Qiu *et. al.* (2007)
Hydrothermal synthesis	Ou and Lo (2007)
Template synthesis	Rattanavoravipa *et. al.* (2008)

2.2.2 Synthesis of TiO_2 Nanotube Arrays via Anodization

Among all the conventional processes for TiO_2 nanostructure synthesis, anodic oxidation, also known as anodization, is the preferred technique. Anodization is widely regarded as a rather straightforward surface treatment technique that can be easily automated to produce TiO_2 nanotubes with decent qualities. Most importantly, anodization does not involve a precursor or a reactant that would possibly induce unnecessary contaminants within TiO_2 nanotubes arrays. Moreover, anodization method is deemed more cost-effective compared to other

electrochemical synthesis techniques because high synthesis temperature and tedious processing protocols are unnecessary (Schmuki *et. al.*, 2006).

The prime reason for producing TiO_2 nanotube arrays using anodization technique is ease of controlling the tube morphologies. TiO_2 nanotubes produced via anodization are highly ordered. They also possess high aspect ratios and are oriented perpendicular to the substrate (e.g., Ti foil). As-anodized TiO_2 nanotubes have well-defined pore size, wall thickness, and tube length. Thus, post-treatment required by other techniques is unnecessary. In modern high-end applications that require uncompromised precision in terms of shape and dimension, synthesis of well-aligned nanotube arrays are necessary. This objective could be achieved through anodization using a metal substrate.

The set up for metal anodization is simple. Only a few important constituents are involved: anodization electrolyte, metal substrate, and counter electrode. Figure 2.2 illustrates a typical anodization setup to produce TiO_2 nanotube arrays. The setup involves two electrodes immersed in an electrolyte that serves as the medium for ion transportation. The working electrode (anode), which is the Ti metal substrate where the TiO_2 formed, is separated from the counter electrode (cathode) at a distance, connected only through an external circuit to a power supply. Upon voltage application, the anode surface area revealed to the electrolyte is oxidized to form an oxide layer. The oxidation process occurs following Reactions 2.1–2.3.

$$M \rightarrow M^{4+} + 4e^{-} \quad (2.1)$$

$$M^{4+} + H_2O/4OH^{-} \rightarrow M(OH)_4 \rightarrow MO_2 + 2H_2O \quad (2.2)$$

$$M(OH)_4 \rightarrow MO_2 + 2H_2O \quad (2.3)$$

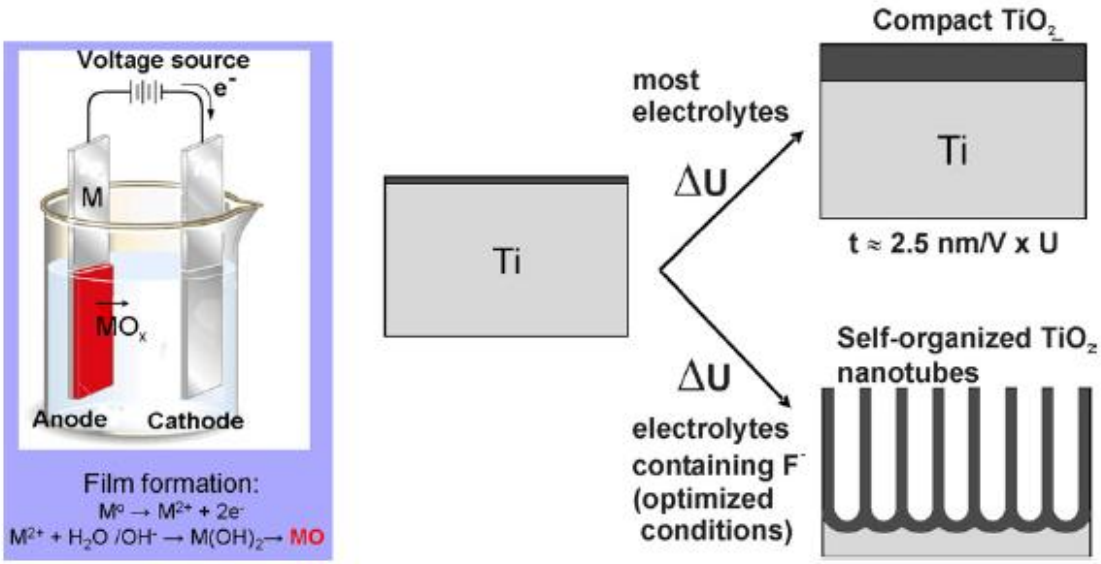

Figure 2.2: Schematic setup for anodization experiment. Anodization leads to oxidation of metal species that form solid oxide on the metal surface. Depending on the anodization conditions, the solid oxide layer can either be compact or nanotubular (Macak *et. al.*, 2007).

The structure of the oxide formed is mostly determined by the electrochemical condition of the anodization process. The oxide layer formed could appear in either compact or nanotubular structure, depending on the anodization parameters. Table 2.3 summarizes the trend of anodization developments. Since the introduction of TiO_2 nanotubes by Hoyer (1996), the development of TiO_2 nanotubes has been revolutionized and could be distinguished into three different stages (Table 2.3). These generations are not differentiated by either the technique nor the approach; rather, changes in the nature of the anodization electrolyte set these generations apart.

Table 2.3: Different stages in the revolution of synthesis of TiO_2 nanotubes.

Stage	Condition
First generation	Utility of aqueous solution containing hydrofluoric acid (HF) or HF electrolytes
Second generation	Utility of buffered neutral electrolytes containing sodium fluoride (NaF) or ammonium fluoride (NH_4F) with pH modification
Third generation	Utility of water free organic electrolytes

2.2.3 Cathode Material for Anodization Process

In the development of anodization technology, the effect of anodization parameters on TiO_2 nanotube arrays has been widely reported. However, to date, published studies on the effect of cathode material used in the anodization process on the features of TiO_2 nanotube arrays formed remain rare. Until recently, only Allam and Grimes (2008) reported on this issue.

Allam and Grimes (2008) studied the effect of some cathode materials obtained from different locations in the periodic table on the morphology of the fabricated TiO_2 nanotube arrays in both aqueous and ethylene glycol electrolytes containing NH_4F and phosphoric acid. The selected cathode materials were divided to platinum (Pt)-group, non-Pt transition, and nontransition elements. The different cathode materials impose different effects on tube structure, dimension, uniformity, and surface morphology. The biggest contribution of the above study was a comparison of cathode stability made of different cathode materials from the three groups.

Allam and Grimes (2008) also reported that certain materials, such as nickel (Ni), could synthesize comparable TiO_2 nanotube arrays to those using Pt as cathode electrode. However, the anodization process consumes a great amount of Ni, and the Ni cathode wears off very quickly. In contrast, materials such as cobalt (Co) have better stability in the long run. However, this attribute has been offset by poorly synthesized TiO_2 nanotube arrays. In addition to Pt, palladium (Pd) also has good stability and could synthesize decent TiO_2 nanotube arrays. However, Pd is a rare and precious material, and would cost as much as Pt. Thus, mass production would not be cost-efficient.

Recently, Tan and Mohamad (2010) reported the synthesis of zinc oxide (ZnO) via zinc (Zn)-air system. Zn-air system is normally utilized as a powering source for applications, such as stationary generators, electrical buses, hearing aids, and others (Neburchilov *et. al.*, 2009), of which ZnO is formed as a byproduct during the application. The successful synthesis of metal oxide employing air-cathode has created the possibility of applying the same concept in anodization process. Considering that the operating condition in metal-air is very similar to the anodization process (i.e., both are considered electrochemical systems), presumably, air-cathode could potentially replace Pt as the cathode material during anodization process.

Though carbon electrode has been studied previously for the synthesis of TiO_2 nanotube arrays, the resulting tube properties are far from ideal (Allam and Grimes, 2008). The commercial air-cathode consists of a metal mesh, porous gas diffusion layer, and catalyst layer, as shown in Figure 2.3. The metal mesh in the air-cathode serves as the current collector of the system, whereas the gas diffusion layer normally comprises carbon layer. The catalyst layer, the most important constituent

in air-cathode, is normally made of activated carbon layer. It is also the catalyst that makes air-cathode prevail from carbon electrode. The function of catalyst layer is to reduce ambient oxygen gas to oxygen ion, react with the metal anode, and form metal oxide more efficiently. The possible metal oxide formation employing air-cathode is shown in Reactions 2.4 and 2.5 (Mohamad, 2006; Deiss *et. al.*, 2002).

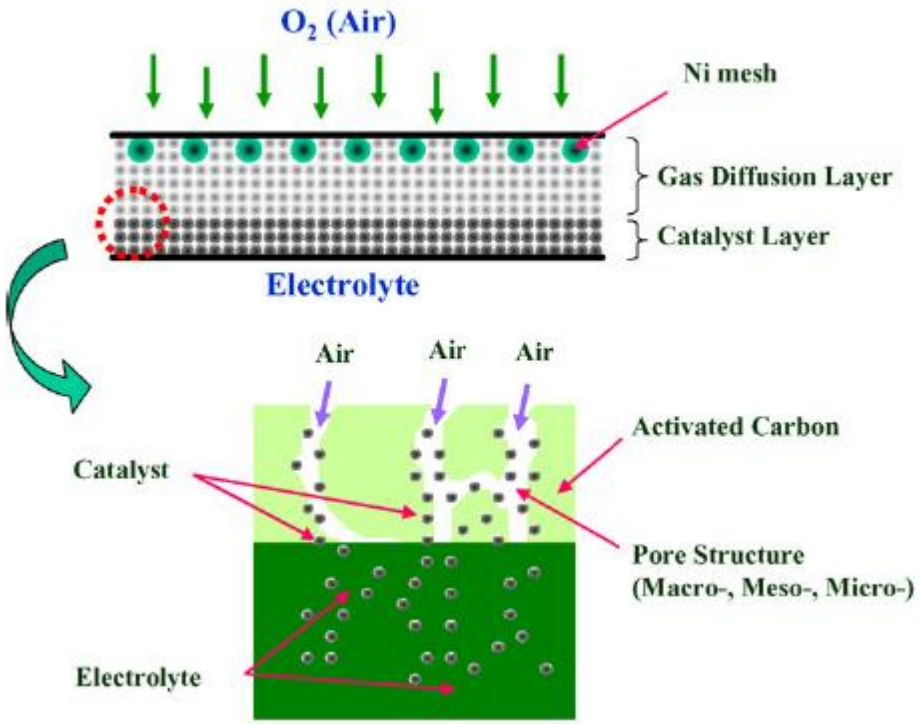

Figure 2.3: Schematic diagram of a commercial air-cathode (Eom *et. al.*, 2006).

At air-cathode:

$$2OH^- \rightarrow \frac{1}{2} O_2 + H_2O + 2e^- \quad (2.4)$$

At anode:

$$M + O_2 \rightarrow MO_2 \quad (2.5)$$

Theoretically, air-cathode has an infinitely useful life and good physical size. Depending on the requirement, the dimensions and the shapes of air-cathode could be altered to suit the desired application. Moreover, air-cathode has high stability, where the physical and electrochemical properties remained unchanged throughout the process (Mohamad, 2006). The other advantage of air-cathode is its cost-effective design. All the constituents involved in air-cathode fabrication are non-precious materials (Neburchilov *et. al.*, 2010).

A cathode material should have the ability to produce decent TiO_2 nanotube arrays without compromising too much on the stability of the cathode material. Studies on cathode stability are insufficient, considering that anodization is normally performed in harsh condition for a considerable period. Cathode performance will deteriorate over the long term. The prime concern for industrialists is how long these cathodes would last without compromising too much on the anodization process. During anodization, the metal ions from the cathode are incorporated into the TiO_2 nanotube array lattice, altering the band gap energy of TiO_2. Thus, it is possible to perform *in situ* band gap engineering on TiO_2 nanotube arrays to enhance their properties for certain applications (Allam and Grimes, 2008).

2.2.4 Growing Mechanisms of TiO_2 Nanotube Arrays

The anodization electrolyte mainly consists of acidic solution. One important component within the electrolyte is singled out: fluoride ions (F^-). The presence of F^- within the electrolyte determines the final structure of the oxide layer. Here, F^- plays a major role in forming the porous/tubular structure on the oxide layer. To fully utilize the advantage of TiO_2 nanotubes, a thorough understanding of tube

formation mechanism and morphology determining factors is essential. Choi, Zhao, Macak, Schmuki, Mor, and Grimes *et. al.* are the leading researchers who proposed the mechanisms of TiO_2 nanotubes formation. Zhao *et. al.* (2005) tried to explain TiO_2 nanotube-forming mechanisms based on understanding of porous alumina formation via anodization. However, the growth mechanisms for the two subjects are not quite similar.

The TiO_2 nanotube formation process requires chemical reaction on the passive Ti substrate. Macak *et. al.* (2007) and Mor *et. al.* (2006) shared a rather similar approach, suggesting that the anodic growth of TiO_2 compact oxide layer on Ti substrate and the formation of TiO_2 nanotubes are governed by a competition between anodic oxide formations, according to Reaction 2.6

$$Ti + 2H_2O \rightarrow TiO_2 + 4H^+ + 4e^- \quad (2.6)$$

and chemical dissolution of the oxide as soluble fluoride complexes, according to Reaction 2.7.

$$TiO_2 + 6F^- + 4H^+ \rightarrow [TiF_6]^{2-} + 2H_2O \quad (2.7)$$

During the Ti oxidation process, the Ti^{4+} ions will react with O^{2-} ions to form an oxide layer. Subsequently, the oxide layer will grow and become controlled by field-aided ion transport ($Ti^{4+}$and O^{2-} ions) through the growing oxide. Apart from TiO_2 formation, a loose and porous hydroxide layer will also precipitate in the previously formed TiO_2 layer (Hahn *et. al.*, 2007). This process is self-limiting and will be terminated once the oxide layer is sufficiently thick to prohibit the current flow. The schematic diagram in Figure 2.4a illustrates the formation of TiO_2 and Ti oxyhydroxide layer.

However, with the presence of F^- ions, the entire process will be different and less straightforward. The presence of F^- ions is the determining factor that ensures the transformation of TiO_2 to a soluble fluoride complex of $[TiF_6]^{2-}$. When the Ti^{4+} ions diffuse through the oxide layer reaching the oxide/electrolyte interface, it will form soluble $[TiF_6]^{2-}$, according to Reaction 2.8. Otherwise, Ti^{4+} can also directly form $[TiF_6]^{2-}$, according to Reaction 2.7.

$$Ti^{4+} + 6F^- \rightarrow [TiF_6]^{2-} \quad (2.8)$$

The small ionic radius of $[TiF_6]^{2-}$ driven by the applied field enable it to slip through the TiO_2 lattice. Thus, permanent chemical dissolution on the TiO_2 layer will occur as long as the field is applied and prevents Ti oxyhydroxide precipitation. Figure 2.4b illustrates the role of F^- in the TiO_2 nanotube-forming mechanisms.

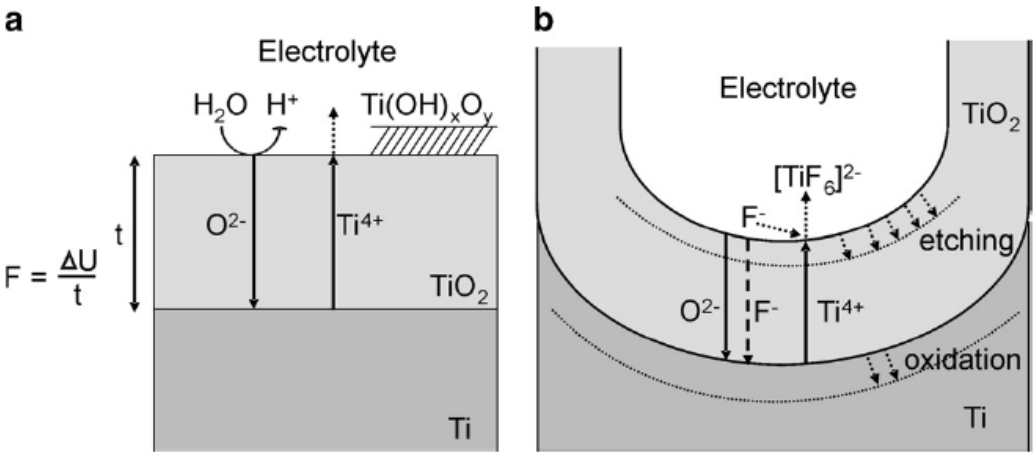

Figure 2.4: Schematic representation of Ti anodization (a) in the absence of fluorides (results in flat layers) and (b) in the presence of fluoride (results in tube growth) (Macak *et. al.*, 2007).

To gain better understanding of actual TiO_2 nanotube array-forming mechanisms, SEM images were taken at different durations of the anodization process (Paulose *et. al.*, 2006), as illustrated in Figure 2.5. As voltage is applied to the system, the anodization process begins. A uniform layer of oxide (approximately 50 nm) forms, spreading across the surface (Figure 2.5a) in just a few seconds, according to Reaction 2.6. Initially, field-assisted oxide dissolution dominates due to the relatively large electric field across the thin oxide layer. Thus, small pits/slits form on the oxide layer (Figure 2.5b) because of localized oxide dissolution, according to Reaction 2.7. At this stage, the barrier layer at the bottom of the pits is relatively thin, which in turn increases the electric field intensity across the remaining barrier layer. As time goes by, these small pits/slits develop and convert to bigger pores. Pore density increases as well (Figure 2.5c).

The pores slowly spread uniformly over the surface and continue to develop and grow (Figure 2.5d). Eventually the whole system arrives at a stage where the rate of oxide growth at the metal/oxide interface and the rate of oxide dissolution at the pore-bottom/electrolyte interface ultimately become equal. Thereafter, the thickness of the barrier layer remains constant, although it moves further into the metal, making a deeper pore. There are small pits formed in the interpore regions as well. The pits formed at this region will develop and eventually lead to pore-separation, yielding individual tube formation (Figure 2.5e).

Choi *et. al.* (2004) adopted a different approach in the growing mechanism of TiO_2 nanotube arrays. They proposed that the growth of TiO_2 nanotube arrays is closely related to the crystallite structure initiated from the oxide formation of Ti. They suggested that porous TiO_2 are formed above the breakdown potential of the oxide. The tube formation mechanisms are illustrated in Figure 2.6. Initially, the

thickness of dense Ti barrier layer increased with increased anodizing voltage. The structure then underwent transitions from amorphous to crystalline oxide (Figure 2.6a).

As anodization continuous, the dense oxide layer induces compressive stress within the oxide. Subsequently, the Ti barrier layer breaks down, and new pores are formed between crystallites (Figure 2.6b). However, the areas where breakdown occurs will be immediately reoxidized (Figure 2.6c). Finally, the inner repassivated pores will again undergo breakdown. The growing structure mimics a cylindrical tube forming TiO_2 nanotube arrays (Figure 2.6d).

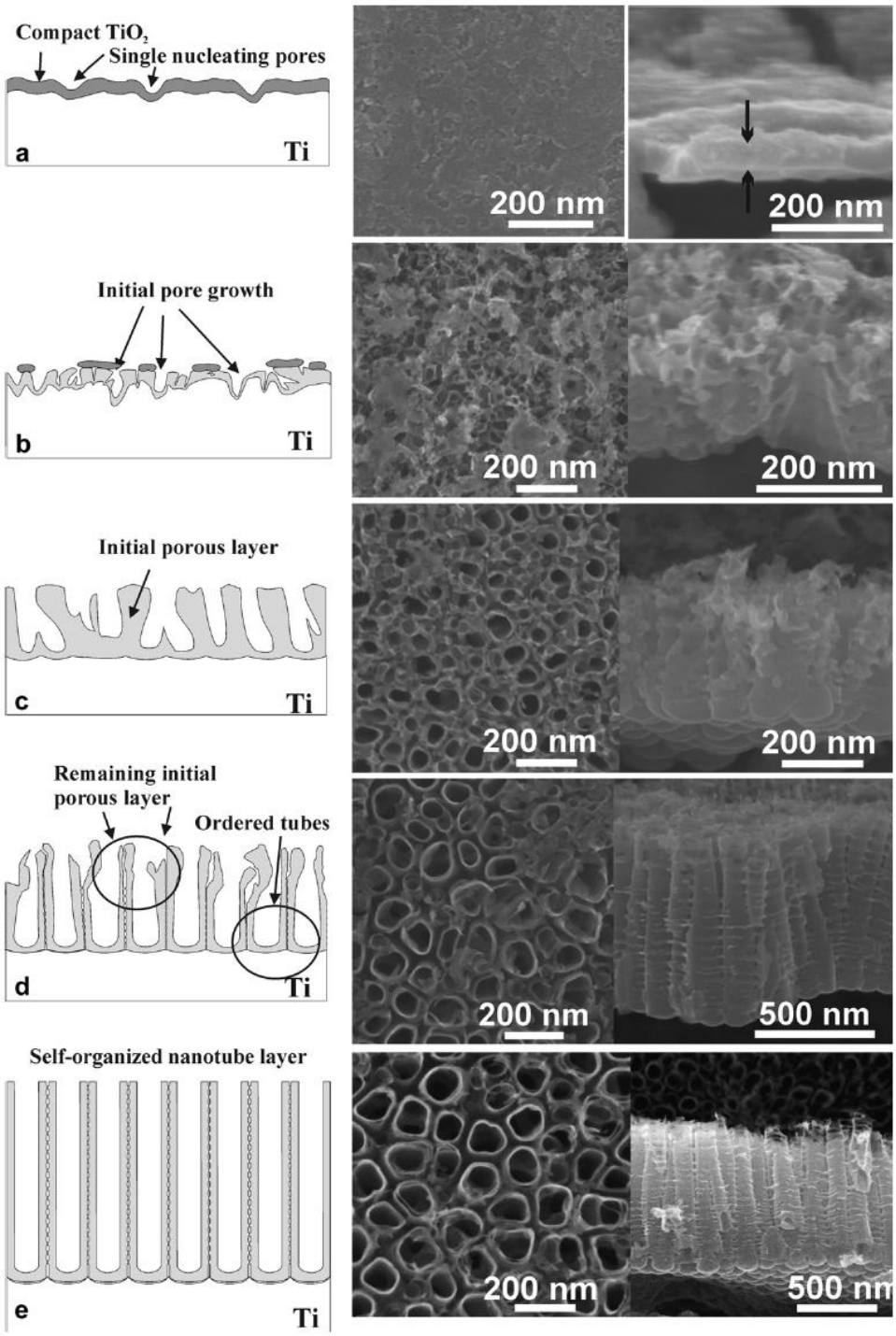

Figure 2.5: Schematic (left column) and SEM sequence (top-views – middle column, cross-sections – right column) of different stages of the TiO_2 nanotube layer formation. Anodization stopped after (a) 0, (b) 3, (c) 10, (d) 30, and (e) 60 min from reaching 20 V in water/glycerol/0.27 M NH_4F after potential ramp from 0 to 20 V, with a sweep rate of 250 mV s^{-1} (Macak *et. al.*, 2007).

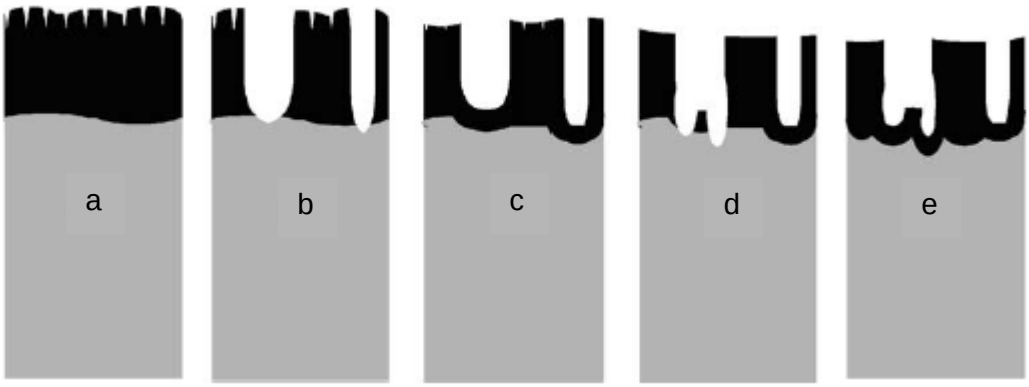

Figure 2.6: Schematic of porous titanium oxide formation above the breakdown potential: (a) oxide growth to maximal thickness, (b) burst of oxide by the formation of crystallites (pore formation), (c) immediate repassivation of pore tips, (d) burst of repassivated oxide, and (e) dissolution of the formed oxide and second repassivation (Choi *et. al.*, 2004).

2.2.5. Effect of Anodization Parameters on TiO_2 Nanotube Arrays

The features of TiO_2 nanotube arrays are greatly affected by the anodization parameters. Thus, understanding the effects of these parameters would have on the final TiO_2 nanotube arrays is necessary to tailor desired structure for specific demands of a particular application. Among all the possible structure altering anodization parameters, a few parameters with definitive effect on synthesizing TiO_2 nanotube arrays with good foundation have been considered.

The early methods to grow TiO_2 nanotube arrays were based on electrochemical anodization in HF-containing aquatic acidic electrolytes (first generation anodization). TiO_2 nanotube arrays from this kind of electrolyte are relatively short, ranging from 100–600 nm (Vega *et. al.*, 2008; Yang *et. al.*, 2008) at similar voltage. In addition, the sidewall of the formed TiO_2 nanotubes is rough and contained rings or ripple. Macak and Schmuki (2006) demonstrated that the key to achieve longer TiO_2 nanotubes is by adjusting the dissolution rate of TiO_2. This

could be achieved by controlling the localized acidification at the pore bottom using buffered or neutral electrolyte.

The use of buffered or neutral electrolyte creates an environment with initially free/very limited of H^+ ions. As mentioned in Reaction 2.6, the formation of TiO_2 yields H^+ ions that contribute to chemical dissolution of the oxide layer (Reaction 2.7). Thus, the concentration of H^+ ions would be higher near the metal/oxide interface during the growing process of the TiO_2 nanotubes. The dissolution process at the top of the tube could be halted. Figure 2.7 illustrates the distribution of the H^+ ions at the tube.

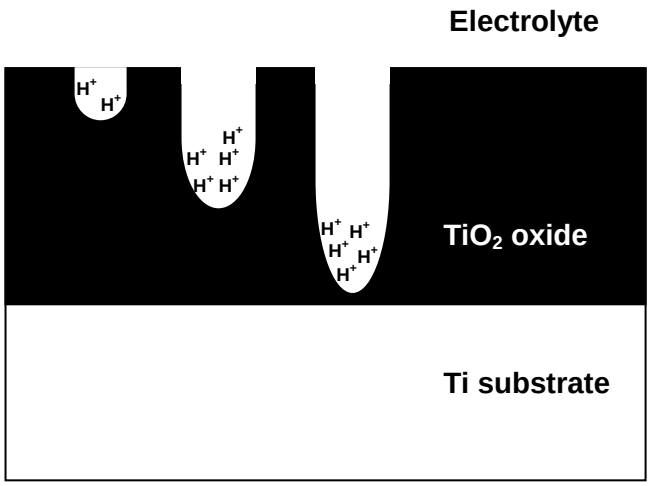

Figure 2.7: Schematic of the distribution of H^+ ions in tubes with different tube depths (Macak and Schmuki, 2006).

Apart from tube length, the viscosity of the electrolyte would affect the sidewall of the TiO_2 nanotube. Figure 2.8 compares the sidewall of TiO_2 nanotubes synthesized using aquatic electrolyte (low viscosity) and organic electrolyte (high viscosity). Yang *et. al.* (2008) reported that the usage of organic electrolyte (high viscosity) could result in smoother wall compared to those achieved using aquatic electrolyte. The formation of ripples on the sidewall of the tube could be attributed to higher diffusivity and concentration of the ions within the aquatic electrolyte. As a result, the high passivation and repassivation rate would induce unstable chemical reaction during tube formation. Breakdown of oxide layer occurs, forming rippled sidewalls.

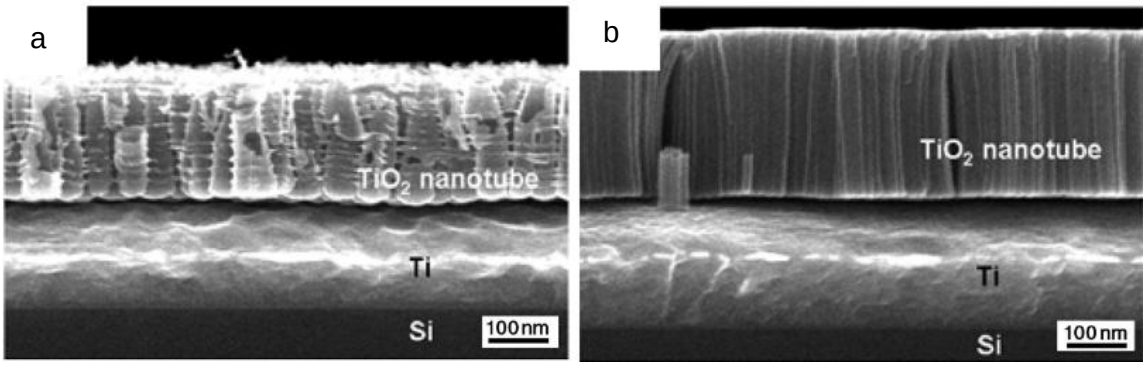

Figure 2.8: SEM micrographs of TiO_2 nanotube sidewall synthesized using (a) aquatic electrolyte and (b) organic electrolyte (Yang *et. al.*, 2008).

The corresponding currents obtained from the Ti anodization process using different aquatic and organic electrolytes are shown in Figure 2.9. Current oscillation, corresponding to the ripple wall formation, is detected on the polarization curve. in contrast, the polarization curve recorded for Ti anodization using organic electrolyte is smooth because of mild ion diffusivity.

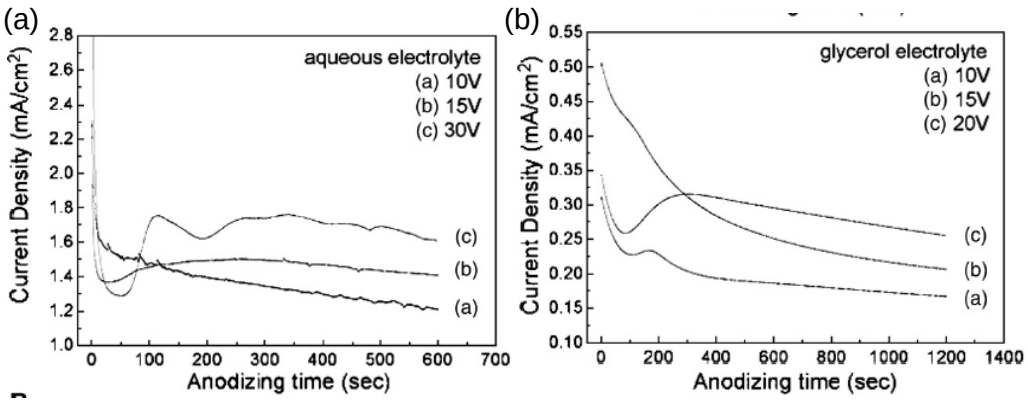

Figure 2.9: Current density-time curves for (a) aqueous electrolyte and (b) glycerol electrolyte (Yang *et. al.*, 2008).

The polarization curves in Figure 2.9 also suggest that the current behavior recorded responds differently towards anodization voltage. The formation of TiO_2 nanotube structure is initiated by localized current that forms pits/slits on the dense oxide layer. The greater the anodization voltage, the greater the size of the pits/slits. The size of the pits/slits formed eventually defines the diameter of the tube formed. Figure 2.10 shows the diameter properties with respect to anodization voltage. Lai *et. al.* (2009) revealed that TiO_2 nanotube diameter is almost proportionate to the voltage applied. Furthermore, there is a minimum voltage required for the TiO_2 nanotubes to grow. Lower voltage would not yield significant tube structure (low length-to-diameter ration) (Figure 2.10a). Subsequently, increasing voltage yields larger tube diameter (Figure 2.10b–d). Figure 2.11 plots the relation between anodization voltage and tube diameter.